On sequential ultrasonic spot welding as an alternative to mechanical fastening in thermoplastic composite assemblies: a study on single-column multi-row single-lap shear joints

Tian Zhao[1], Calvin Rans, Irene Fernandez Villegas*, Rinze Benedictus
Aerospace Structures and Materials Department, Faculty of Aerospace Engineering, Delft University of Technology, Kluyverweg 1, 2629HS Delft, The Netherlands

Corresponding author: I.FernandezVillegas@tudelft.nl

Abstract

In previous work, single-spot ultrasonically welded joints were found to feature similar load carrying capability in shear but significantly low capability in peel as joints with a representative single-mechanical fastener. This leads to questioning welding as an appropriate solution for the commonly-used single-lap joint configuration. The present paper investigates the mechanical performance of spot welded single-lap joints in thermoplastic composites in comparison to their mechanically fastened counterparts. Single-row joints, double-row joints with varying inter-row distance and multi-row joints with varying number of rows were investigated in this study. The results showed that, owing to higher joint stiffness and hence lower secondary bending and peel stresses, the load carrying capability of the spot welded joints was comparable to that of the mechanically fastened joints in all considered cases. Likewise, the effects of increasing the inter-row distance and of increasing the number of rows were similar for both types of the joints.

Keywords: Thermoplastic resin, Mechanical properties, Fractography, Joints/joining

1 Introduction

Thermoplastic composites (TPCs) are becoming increasingly attractive to aerospace and automotive industries as a potential alternative to thermoset composites for their cost-

[1] Institute of Advanced Structure Technology, Beijing Institute of Technology, 100081 Beijing, PR China

effective manufacturing and welding processes, their high damage tolerance and their recyclability [1-3]. Among all the welding techniques applicable to thermoplastic composites, ultrasonic welding is a very interesting process owing to its very high speed, its potential for automation and the absence of foreign materials at the welding interface [4, 5]. One approach to applying ultrasonic welding to large thermoplastic composite assemblies entails the creation of multi-spot welded seams using a sequential ultrasonic welding process. Multi-spot welded seams can be expected to have lower load carrying capability and lower sealing properties than continuous welded seams. Nevertheless sequential ultrasonic welding offers high flexibility and, currently, a higher technology readiness level than continuous ultrasonic welding of thermoplastic composites [6]. Secondly, owing to the obvious similarity between multi-spot welded joints and mechanically fastened joints, design principles traditionally used for the latter might be straightforwardly adapted for the former, easing their introduction in industry. Thirdly, the discontinuous nature of multi-spot welded joints might lead to inherently damage tolerant welded seams when proper design principles are applied.

In order to set the basis for the evaluation of multi-spot sequential ultrasonic welds as an alternative to mechanically fastened joints for thermoplastic composite assemblies, our previous study [7] investigated the load carrying capability of single-spot welded joints and mechanically fastened joints with a single fastener in pure shear and in pure peel loading conditions on carbon fibre reinforced polyether-ether-ketone (CF/PEEK) composites. The main results of that study were the following. Firstly, the single-spot welded joints showed comparable load carrying capability to that of the mechanically fastened joints in pure shear loading conditions. Secondly, owing to the fact that the weld strength entirely relies on the out-of-plane strength of the composite laminate, the load carrying capability of the welded joints when subjected to peel loading amounted to only 20-25% that of the mechanically fastened joints. Thirdly, in the pure shear loading conditions the welded joints were almost

two times as stiff as the mechanically fastened joints. The lower stiffness of the mechanically fastened joints was attributed to the pin load applied by the fastener to the composite laminate. Finally, failure of the welded joints, which took place at the outermost ply of the composite laminates, resulted in significantly less damage in the composite laminate as compared to that involved in the failure of mechanically fastened joints [7]. As these results indicate, spot welded joints could be a plausible composite-friendly alternative to mechanically fastened joints, however joint designs that minimize out-of-plane loading might be desirable or even necessary in (spot) welded assemblies.

One of the most common structural joint designs is the single-lap joint. Despite their simplicity in terms of geometry and manufacturability, single-lap joints exhibit relative complex stresses. When loaded in tension, load transfer across the interface of a single-lap joint should ideally result in shear stresses. However, so-called secondary bending occurs in single-lap joints owing to the eccentricity of the single-lap configuration. Secondary bending results in out-of-plane deformation of the overlap and thus introduces additional peel stresses in the single-lap joints [8-15]. Extensive research, including both numerical and experimental work, has been carried out on the effect of secondary bending on single-lap mechanically fastened joints in metallic [10-12], hybrid [12,13] and composite structures [14,15]. In particular, Schijve proposed a simple 2D analytical model known as “neutral line model” to calculate secondary bending in double-row mechanically fastened joints and showed that secondary bending can be decreased by increasing the inter-row distance [10, 11]. Later on, Müller proposed a modified model which could be applied to multi-row mechanically fastened joints by taking into account the fastener flexibility [12]. Regarding thermoplastic composite welded joints, the single-lap configuration is also the most widely used and tested [4, 5, 16, 17]. There is however very little knowledge on secondary bending in this type of joints and on how the combination of shear and peel stresses affect the ability of the welded joints to carry loads. Dubé et al. [18]

comparatively studied the behaviour of single- and double-lap resistance welded joints in carbon fibre reinforced polyether-ether-ketone composites. Their main result was that the single-lap joints had similar apparent shear strength to the double-lap shear joints. This result could be interpreted as an indication of the absence of significant peel stresses in the single-lap welded joints. However, the presence of dissimilar weld quality between the two welds in the double-lap joints, as suggested by their fractographic analysis, could have resulted in a lack of symmetry and some secondary bending during testing of the double-lap joints.

The experimental research presented in this paper aims at providing further insight into whether sequential ultrasonic spot welding could be regarded as an alternative to mechanically fastening for single-lap joints in thermoplastic composite structures. As an initial step to study sequentially spot welded joints, this research focused on single-lap joints provided with a single column (parallel to load direction) of welded spots or mechanical fasteners. The research was composed of different stages with increasing levels of complexity in which the number of spots or fasteners (i.e. the number of rows) was progressively increased. Firstly, single-row spot welded joints were compared to single-row mechanically fastened joints. Secondly, double-row spot welded joints with different distances between rows were compared to double-row mechanically fastened joints. Thirdly, multiple-row spot welded joints with different numbers of rows were compared to multi-row mechanically fastened joints. In all cases, the thermoplastic composite used was carbon fibre reinforced polyphenylene sulphide (CF/PPS). The welded and mechanically fastened samples were mechanically tested to determine the load carrying capability of the joints as well as their failure modes. Image analysis was used on the fracture surfaces of the welded joints to determine the amount of welded area in each spot. During the mechanical tests, digital image correlation was used to measure the out-of-plane displacement of the overlap and the neutral line model was used to calculate the secondary bending stress.

2 Experimental

2.1 Materials

For the welded and mechanically fastened test specimens, two materials needed to be produced: the thermoplastic composite adherends and a neat thermoplastic resin film to be used as an energy director (ED) during the welding process. Cetex® carbon fibre reinforced polyphenylene sulphide (CF/PPS) with 5 harness satin fabric reinforcement, supplied by Ten Cate Advanced Composites (The Netherlands) as powder-impregnated prepreg, was used to manufacture the thermoplastic composite adherends. Laminates made out of six prepreg plies with dimensions 580 mm x 580 mm and $[0/90]_{3s}$ stacking sequence were consolidated in a hot-platen press at 320 °C and 1 MPa for 20 min. The final thickness and the nominal fibre volume fraction of the resulting laminates were 1.90 mm and 58 %, respectively. A water-cooled diamond saw was used to cut the laminates into 25.4 mm-wide adherends of different lengths as listed in Section 2.3. The adherends were cut such that the main apparent fibre orientation on their outer surfaces was parallel to their longer side (i.e. loading direction in the single-lap shear test). Additionally, neat Fortron® PPS film of 0.08 mm thickness was used to manufacture flat energy directors used in the welding process to concentrate heat generation at the welding interface [5]. Three PPS layers were stacked together and consolidated in a hot platen press at 260 °C and 2 MPa for 10 min to manufacture 0.24 mm-thick flat ED sheets.

It should be noted that the material of the adherends was different than the one used in [7]. This change resulted from the fact that the power required to weld the CF/PEEK adherends used in [7] following the specific welding procedure used in the present paper (and described in the following section) exceeded the (rather limited) maximum power that the ultrasonic welder used in the present study was able to deliver.

2.2 Assembly techniques

Sequential ultrasonic welding using a 20 kHz Rinco Dynamic microprocessor-controlled ultrasonic welder with a maximum power output of 3000W was used to obtain the multi-spot welded joints. A 10 mm-diameter-circular sonotrode was utilized to create the individual spots in the welded joints. Flat energy directors cut into 4 mm diameter circles were manually placed on the bottom adherend at each intended spot weld location prior to the welding process. Each energy director was tacked in place with the help of a Rinco handheld ultrasonic welder. Both the upper and lower adherend (already provided with the energy directors) were clamped with two aluminium bars to a base plate with a 20 Nm torque (Figure 1). The upper adherend partially rested on the lower adhered (single lap overlap area) and on a 1.8 mm-thick aluminium supporting plate. This configuration introduced a small misalignment between the surfaces of the adherends which was nevertheless corrected once the sonotrode applied pressure on the overlap. This thin, 1.8 mm-thick, base plate was selected to allow for unobstructed downward movement of the sonotrode during melting and flow of the energy director. After welding of each individual spot, the sample was manually unclamped, shifted and clamped again to weld the next spot.

Regarding the welding process, displacement-control was used as the welding control strategy. In other words, the vibration applied into the welding stack was stopped when a pre-defined vertical displacement of the sonotrode was achieved. The welding parameters were defined based on previous results reported in [19]. In particular, the peak-to-peak vibration amplitude was set to 60.8 µm and the welding force was set to have an initial value of 1500 N (onset of the vibration) and to linearly increase at a rate of 1000N/s during the vibration phase. For these amplitude and force values, a sonotrode displacement of 0.23 mm was used to obtain high quality welds. Once the vibration was stopped, the welds were kept under 1500 N force for 4 s for solidification. Owing to the flow of molten energy director during the

welding process, the final diameter of each welded spot was around 10 mm. It should be noted that displacement-controlled welding was selected for this study with the goal of obtaining consistent weld quality in each one of the spots of multi-spot welded joints produced with a unique set of welding parameters [19].

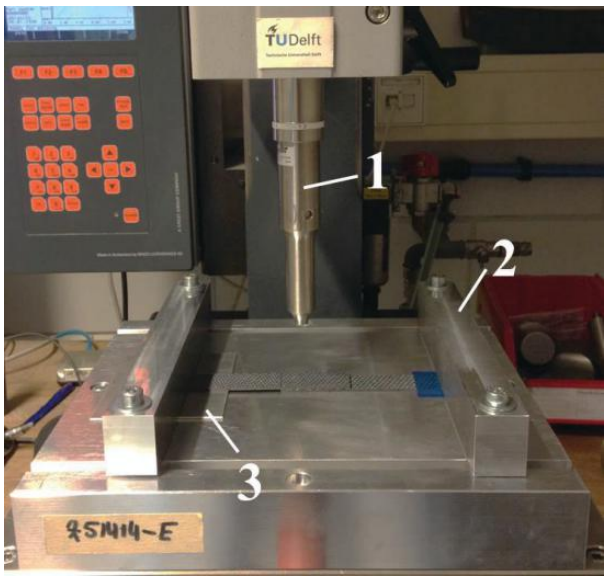

Figure 1. *Ultrasonic welder and welding jig used in this study. 1: sonotrode, 2: bar clamp, 3: supporting plate for the upper adherend.*

In the case of the mechanically fastened CF/PPS joints, titanium HL10V6 Hi-Lok® fasteners with a protruding head were used. The pin length and diameter were 4.0 and 4.8 mm, respectively. The diameter of the fasteners was selected to be in the range of 2.5-3 times the thickness of the thickest joined part. Clearance holes were drilled in the composite adherends prior to the installation of fasteners. During drilling, a wooden support was used to minimize the risk of delamination in the composite adherends during tool entry and exit [20]. Fasteners were manually installed with a ratchet wrench, following the procedure recommended by the fastener manufacturer [21]. It should be noted that the fastener contains a collar that shears off once the appropriate installation torque is reached, ensuring a consistent installation and fastener clamping force between the various installed fasteners.

2.3 Test design and test procedure

As mentioned earlier, three different types of single-column spot welded and mechanically fastened joints were tested in this study: single-row joints (with only one welded spot or fastener), double-row joints (with two welded spots or fasteners) and multi-row joints (with more than two welded spots or fasteners). Figure 2 shows a schematic of a generic sample and Table 1 lists the main characteristics and dimensions of all the spot welded and mechanically fastened joints in this study. In the double-row joints the inter-row distance and hence the overlap length were varied in order to investigate the effect of secondary bending on the performance of the joints. Note that the free-sheet length was varied along with the inter-row distance to avoid any constraints that a too short free-sheet length might impose on secondary bending of the overlap during the mechanical tests [10]. In the multi-row joints, the overlap length was kept constant to mainly focus on the effect of increasing row number on load distribution among the rows. Consequently the inter-row distance decreased with increasing number of rows.

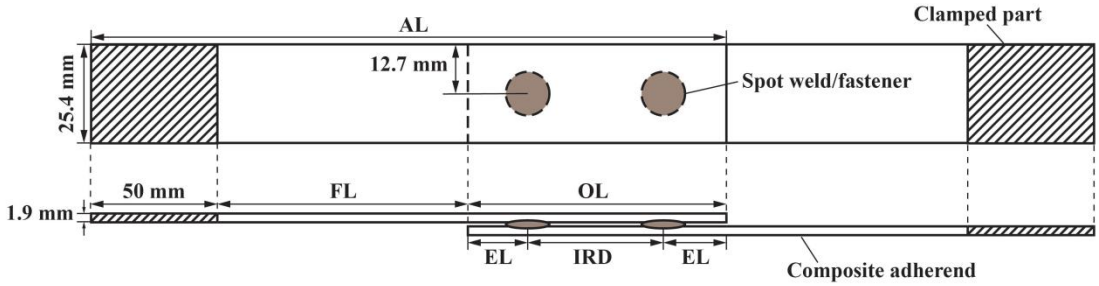

Figure 2. *Schematic of the generic configuration of single lap shear joint specimen in this study. Dimensions are not to scale. AL: adherend length, OL: overlap length, IRW: inter-row distance, EL: distance to edge, FL: free sheet length.*

Single lap shear tests were performed in Zwick/Roell 250 KN universal testing machine equipped with hydraulic grips which were offset to ensure parallelism between the load path and the joint interface. Tests were initiated with a preload of approximately 100 N and performed at a constant crosshead speed of 1.3 mm/min. Five samples were tested for each joint configuration. In the case of the welded joints, which feature brittle behaviour [7], the

ultimate failure load (UFL) was considered as the indicator of the load carrying capability of the joint, denoted as LCC hereafter. In the case of mechanically fastened joints, the LCC was linked to the onset failure load (OFL) since it indicates the onset of critical failure mode in the adherends [22]. The onset failure load of the mechanically fastened joints was calculated using a bilinear approximation [7,23] on the load displacement curves obtained from the mechanical tests, as shown in Figure 3. Note that, contrarily to usual procedure in studies on composite welded joints, the LCC and not the strength of the welded joints (calculated as the total load divided by the welded area) was used in this study in order to ease the comparison with the mechanically fastened joints. The total amount of welded area in the spot welded joints was nevertheless measured to detect potential irregularities in the welding process [7]. Measurement of the welded area was performed using the image analysis software Image150 (NIH) ImageJ150 (NIH) on fracture surface images taken with a Zeiss stereo-microscope. As indicated by the example shown in Figure 4, the flow front of the energy director was not considered when measuring the welded area since it featured adhesive failure and hence its contribution to the weld strength was assumed to be negligible. In other words, only the area which showed failure within the composite adherends was considered as the welded area.

Table 1. *Relevant data for different types of spot welded (SW) and mechanically fastened (MF) joints in this study. AL: adherend length, OL: overlap length, EL: distance to edge, FL: free sheet length, IRD: inter-row distance (see Figure 2)*

Joint reference		Number of rows	AL (mm)	OL (mm)	EL(mm)	FL (mm)	IRD (mm)
1SW	1MF	1	110.0	25.4	12.7	34.6	-
		2	130.0	40.0	15.0	40.0	10.0
2SW	2MF	2	150.0	50.0	15.0	50.0	20.0
		2	170.0	60.0	15.0	60.0	30.0
		2	190.0	70.0	15.0	70.0	40.0
3SW	3MF	3	190.0	70.0	15.0	70.0	20.0
4SW	4MF	4	190.0	70.0	15.0	70.0	13.3

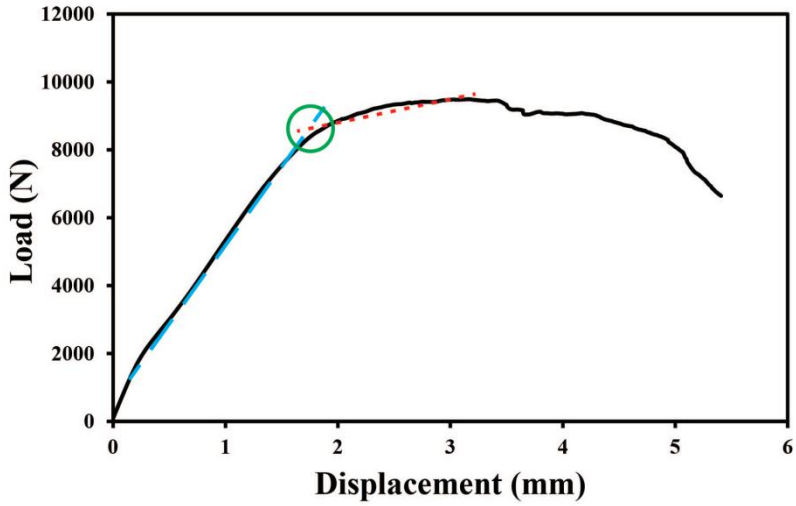

***Figure 3**. Bilinear approximation (dashed lines) to determine the onset failure load of a double-row mechanically fastened joint. The onset failure load, considered in this study as the load carrying capability of the joint, is indicated by the circle at the intersection of two fitting lines.*

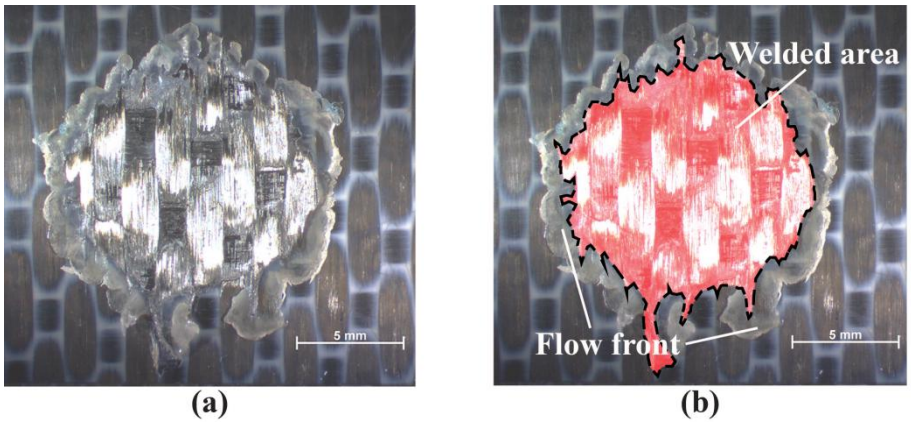

***Figure 4.** (a) Representative fracture surface of spot welded joint and (b) calculation of the WA (highlighted by the red area surrounded by the dashed line). The flow fronts surrounding the welded area are not taken into account for the calculation in the assumption of negligible contribution to the weld strength.*

During mechanical testing, the Vic-3D digital image correlation (DIC) system, supplied by Limess Messtechnik & Software GmbH Inc, Germany, was used for measuring the out-of-plane displacement of the joint overlap as shown in Figure 5a. Two CCD (charge coupled device) cameras combined with a light source were utilized to digitally track the random dot pattern applied on the surface of the samples during the loading process [13, 24]. The top surface of the overlap, instead of the edge of the sample, was chosen for the observation of secondary bending as shown in Figure 5b. The position of the cameras relative to each other and to the

testing machine was established through a calibration process in order to ensure that the measurements were accurate enough for the purpose of this research. Prior to the tests, the surfaces to be tracked were cleaned with alcohol and spray-painted to get a high-contrast pattern consisting of random black speckles on a white background. Images of the speckle pattern were captured at a frequency of 1 Hz during the tests. The first image was taken prior to the starting of the mechanical test and it was used as reference to calculate the cumulative strain on the tracked surface.

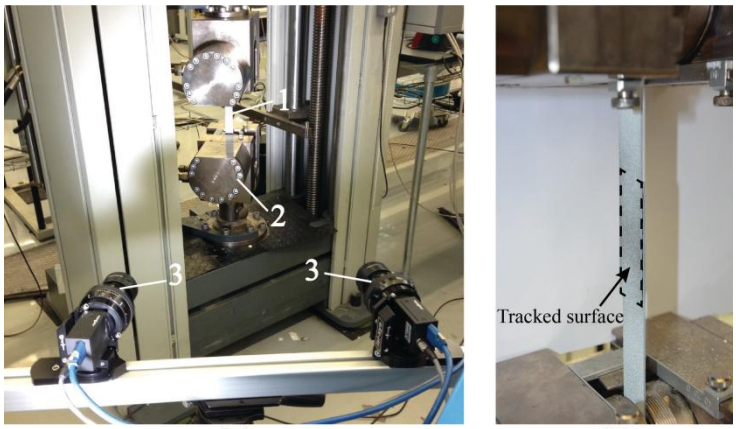

(a) (b)

Figure 5. *(a) Mechanical test set-up: 1, specimen, 2, hydraulic grips, 3, CCD cameras, and (b) the magnification of testing specimen. The area framed by dashed line indicates the surface being tracked during tests.*

2.4 Neutral line model

The neutral line model proposed by Schijve [10], was used in this study to calculate the bending stress at the location of the welded spots or fasteners and the out-of-plane deformation of the joint overlap in the double-row joints. This model has been widely used in calculations for different types of mechanically fastened joints [10-12], however its applicability to spot welded joints is yet unknown. Figure 6a shows the neutral line of a double-row mechanically fastened joint indicating the eccentric load path. According to this, the load path is transferred from the centre line of one adherend to the interface of the joint through one of the fasteners and then back to the centre line of the other adherend through the other

fastener. As also indicated in Figure 6a, each half joint can be considered to be composed of two parts: part I, from the free edge of the adherend to the first fastener, and a part II, from the first fastener to the middle of the overlap. Part I is modelled as a beam with the same thickness as the adherend subjected to a combination of a tensile load and a bending moment due to the load eccentricity. Part II is modelled as a beam with the combined thickness of the two adherends also subjected to a combination of a tensile load and a bending moment (Figure 6b). Secondary bending can be calculated by considering the equilibrium of bending moments, as shown in Figure 7. According to the beam theory, bending moments for both part I and part II (M_{xi}) can be calculated using the following equation:

$$M_{xi} = E^{*} I_i (\frac{d^2 w}{dx^2})_i \qquad [1]$$

where E^{*} is the Young's Modulus for plane bending of 2D model:

$$E^{*} = \frac{E}{(1-v^2)} \qquad [2]$$

where E and v are the Young's modulus and the Poisson ratio of the material, respectively (55.8 GPa and 0.33, respectively, according to the data sheet provided by the material supplier [25]). I is the moment of inertia of the cross section of the beam and w is the out-of-plane deformation of the neutral line. For each part of the beam, I can be calculated as: $I_1 = \frac{Wt^3}{12}$ and $I_2 = \frac{W \cdot (2t)^3}{12}$, where W and t are the width and thickness of the laminate, respectively. W could be assumed to be one for the 2D model, while t was 1.9 mm as indicated in Section 2.1. Finally, the bending stress (S_b) at each one of the two fasteners is given by:

$$S_b = \frac{M_{(x_1 = L_1)}}{Wt^2 / 6} \qquad [3]$$

Regarding the application of the neutral line model to the joints considered in this study, the following should be taken into account. First, the effect of the offset grips was input in the neutral line model calculation as 1.9 mm misalignment (equal to the adherend thickness) in the applied load [10]. Second, in the neutral line model the connections between the two adherends are simplified as rigid and infinitely thin lines, which was not exactly the case for either the mechanically fastened or the spot welded joints. Third, owing to experimental difficulties in measuring the flexibility of mechanically fasteners and, in particular, of the welded spots, secondary bending in multi-row (i.e. three and four rows) joints was not theoretically analysed in this study.

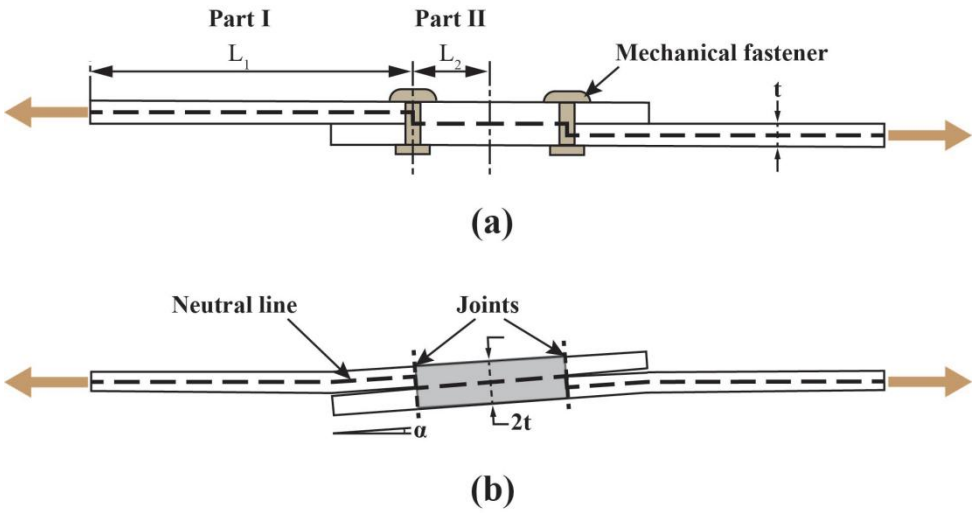

Figure 6. *Eccentric loading path and neutral line within single lap joints: (a) double-row mechanically fastened joint; (b) neutral line as affected by secondary bending. The rotation angle of the overlap is indicated as α.*

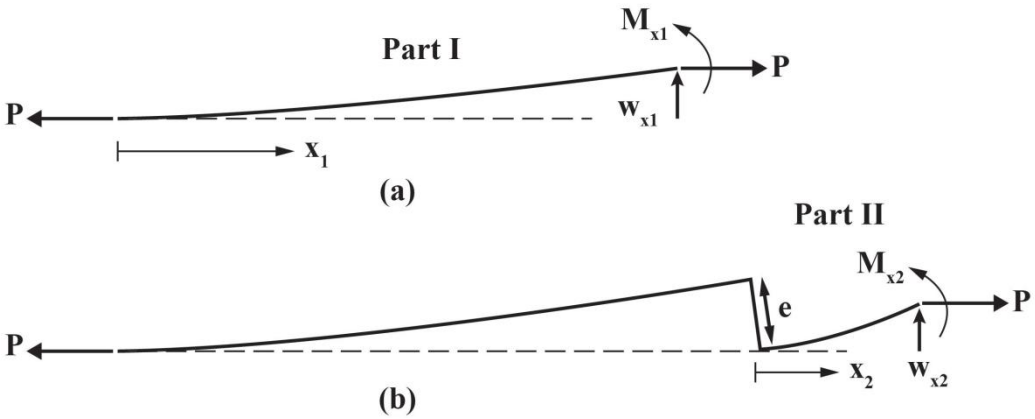

Figure 7. *Force and moment diagrams for the two parts in which half of the joint is divided according to the neutral line model: (a) Part I: from adherend free edge to first fastener; (b) Part II: from first fastener to middle of the overlap. The eccentricity is indicated by "e".*

3 Results and discussion

3.1 Single-row single lap joints

Figure 8 shows representative load displacement curves for a single-row spot welded joint and for a single-row mechanically fastened joint. As seen in this figure, the ultimate failure load (UFL) of the spot welded joint was lower but not far from the onset failure load (OFL) of the mechanically fastened joints. The average values corresponding to the five samples tested per joint type are shown in Table 2. These results indicate that, contrarily to our expectations built upon the poor performance of spot welded joints under pure peel loading [7], the tensile load carrying capability of single-row spot welded single lap joints was comparable (around 10% lower) to that of single-row mechanically fastened single lap joints. This behaviour might be explained by the significantly higher stiffness of the spot welded joints, as seen in Figure 8 and also in [7]. This higher joint stiffness could be expected to result in significantly lower secondary bending and hence significantly lower peel stresses in the welded joint as compared to the mechanically fastened joint. It should be noted that the significant lower stiffness of the mechanically fastened joints could be attributed to the pin load introduced in the composite by the fastener [7] and to the fastener rotation observed during the single-lap shear tests. Another interesting observation from the tests on single-row joints was that the spot welded joints experienced sudden failure (first ply failure in the composite adherends, as also observed in [7]) whereas the mechanically fastened joints underwent gradual failure (fastener rotation and pull out). The actual welded area in the single-row spot welded joints as measured on the fracture surfaces amounted to 92.6 ± 2.9 mm^2, which corresponded to a 10.8 mm average spot diameter.

3.2 Double-row single lap joints

Figure 9 and Table 2 summarize the results obtained regarding the load carrying capability of the double-row joints. In Figure 9 the LCC of the single-row joints times two is also shown as

a reference. In general terms the LCC of both the double-row spot welded and mechanically fastened joints increased with increasing inter-row distance, with the former being generally 10% lower than the latter. In the case of the shortest inter-row distance, i.e. 10 mm, the LCC of the spot welded joints was however around 20% lower than the LCC of the mechanically fastened joints. Moreover, also in the case of the shortest inter-row distance the LCC of both the double-row spot welded and mechanically fastened joints was lower than the reference LCC values, i.e. two times the LCC of single-row spot welded and mechanically fastened joints, respectively.

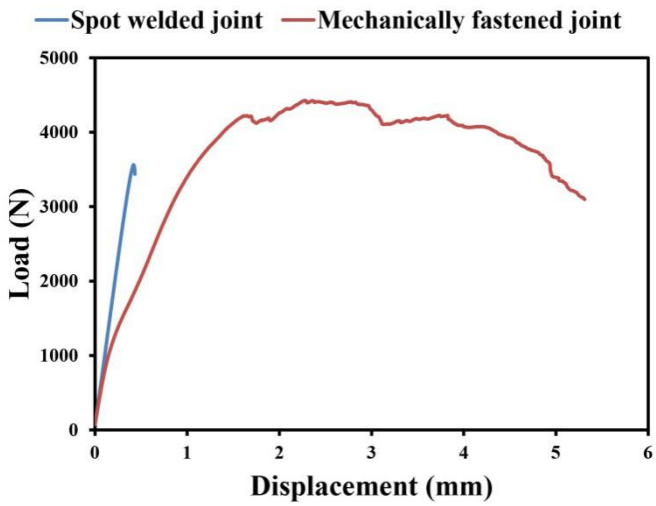

Figure 8. *Representative load versus displacement curves for single-row spot welded and mechanically fastened joints.*

Table 2. *Load carrying capability (average ± standard deviation) of all spot welded (LCC_{SW}) and mechanically fastened (LCC_{MF}) joints obtained in this research. It should be noted that LCC_{SW} refers to ultimate failure load whereas LCC_{MF} refers to onset failure load.*

Number of rows	Inter-row distance (mm)	LCC_{SW} (N)	LCC_{MF} (N)
1	-	3527 ± 239	3919 ± 78
2	10.0	5867 ± 459	7329 ± 304
2	20.0	7049 ± 156	7931 ± 436
2	30.0	7449 ± 122	8195 ± 128
2	40.0	7776 ± 276	8483 ± 144
3	20.0	10272 ± 496	10467 ± 1103
4	13.3	11101 ± 393	11167± 877

The increasing trends observed in Figure 9 for the LCC of both the spot welded and the mechanically fastened joints could be explained by a decrease in the secondary bending of the double-row joints with increasing inter-row distance. Figure 10 shows how, according to the predictions of the neutral line model, the bending factor, i.e. the ratio between the bending and tensile stresses, should experience a non-linear decrease with increasing inter-row distance. However, given the simplifications inherent to the neutral line model, out-of-plane displacement measurements on the overlap of the double-row joints were performed to validate the predictions. Figure 11 shows plots for the out-of-plane displacement along one of the surfaces of the overlap as predicted by (i) the neutral line model, and as calculated from DIC measurements on (ii) the double-row spot welded, and (iii) the double-row mechanically fastened joints. Note that these plots correspond to the same fixed load level (i.e. 5000 N) as the results in Figure 10. From the plots shown in Figure 11 an overall rotation angle of the overlap α (as indicated in Figure 6b) was estimated for all the cases studied by dividing the increment of out-of-plane displacement between the edges of the overlap by the overlap length. The results of this calculation, listed in Table 3, indicate that the rotation angle, and hence secondary bending, decreased with increasing inter-row distance in both the spot welded and the mechanical fastened joints, as predicted by the neutral line model. They also show that in all cases the rotation angle in the spot welded joints was significantly lower than that in the mechanically fastened joints, which is consistent with the higher stiffness of the spot welded joints. These differences also mean that the neutral line model, with a unique solution for both types of joints, was not able to predict bending of the spot welded joints and the mechanically fastened joints with the same level of accuracy. Looking back at Figure 11, it can be indeed seen that the predictions of the neutral line model correlated relatively well with the measurements on the mechanically fastened joints (as already expected from results shown in literature [10-12]). However, there was a significant divergence between the neutral

model line predictions and the DIC measurements on the spot welded joints. This result is related to the way in which the joints are idealized in the neutral line model, i.e. the connections between the adherends are modelled as rigid and infinitely thin lines, so to say, as hinging axes during the bending of the adherends. The local weakening caused in the adherends by the drilled holes in mechanically fastened joints can be expected to have a similar hinging effect, thereby the good correlation between predictions and experimental results despite the finite diameter of the fasteners. That is however not the case in the spot welded joints, where the relatively big size of the welded spots and the lack of holes in the adherends result in much more restricted deformation.

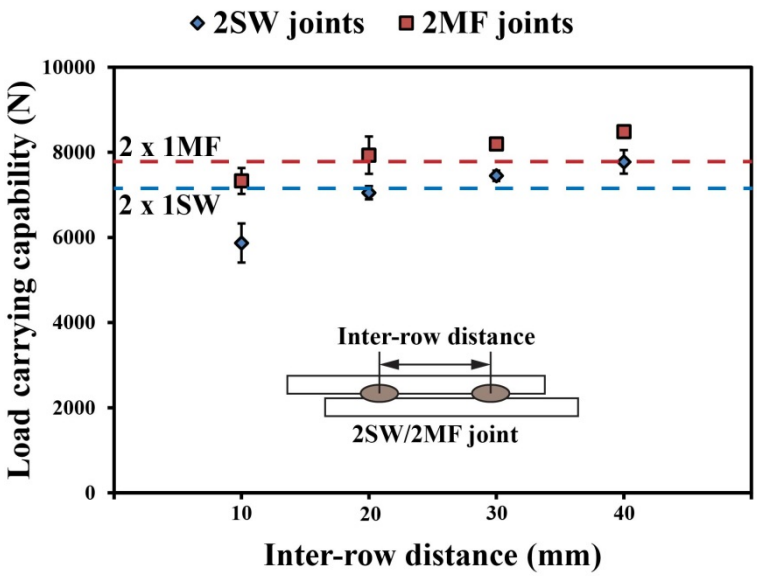

Figure 9. *Load carrying capability of the double-row spot welded and mechanically fastened joints with increasing inter-row distance. Two times the load carrying capabilities of single-row joints are provided as references.*

The apparently abnormal behaviour of the spot welded joints with the shortest inter-row distance could, at least, be partially explained from the measurement of the actual welded areas. Figure 12 and Table 4 show that the average welded area per spot was significantly lower in the case of the shortest inter-row distance (approximately 83% of the average welded area in the single-row spot welded joints). In particular, the area of the first welded spot was

significantly lower than that of the second spot. This was attributed to an interaction between the molten flow of the first energy director and the second intact energy director during welding of the first spot, as shown in Figure 13. Moreover interactions during mechanical testing between either welded spots or fasteners in very close proximity could as well be expected to contribute to the relative LCC values obtained for the shortest inter-row distance in both the spot welded and the mechanically fastened joints. In the case of the mechanically fastened joints proximity between the two fasteners also caused clear differences in the failure mode. As seen in Figure 14, the 10 mm and 20 mm inter-row distances resulted in net section failure through bending of the laminate, whereas the 30 and 40 mm inter-row distances resulted in fastener pull through. No apparent effect of the inter-row distance was however found in the failure mode of the spot welded joints, which featured first-ply failure for all inter-row distance values.

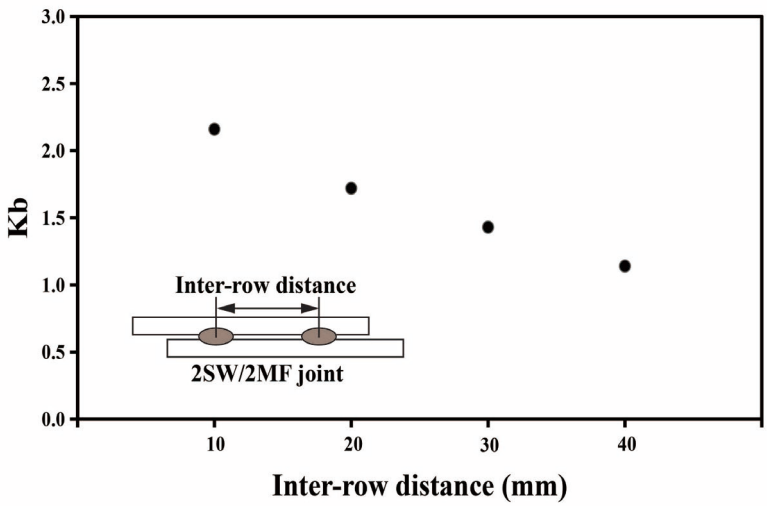

Figure 10. *Bending factor (K_b = bending stress/tensile stress) predicted by the neutral line model as applied to the single lap geometries, adherend materials and inter-row distances studied in this paper.*

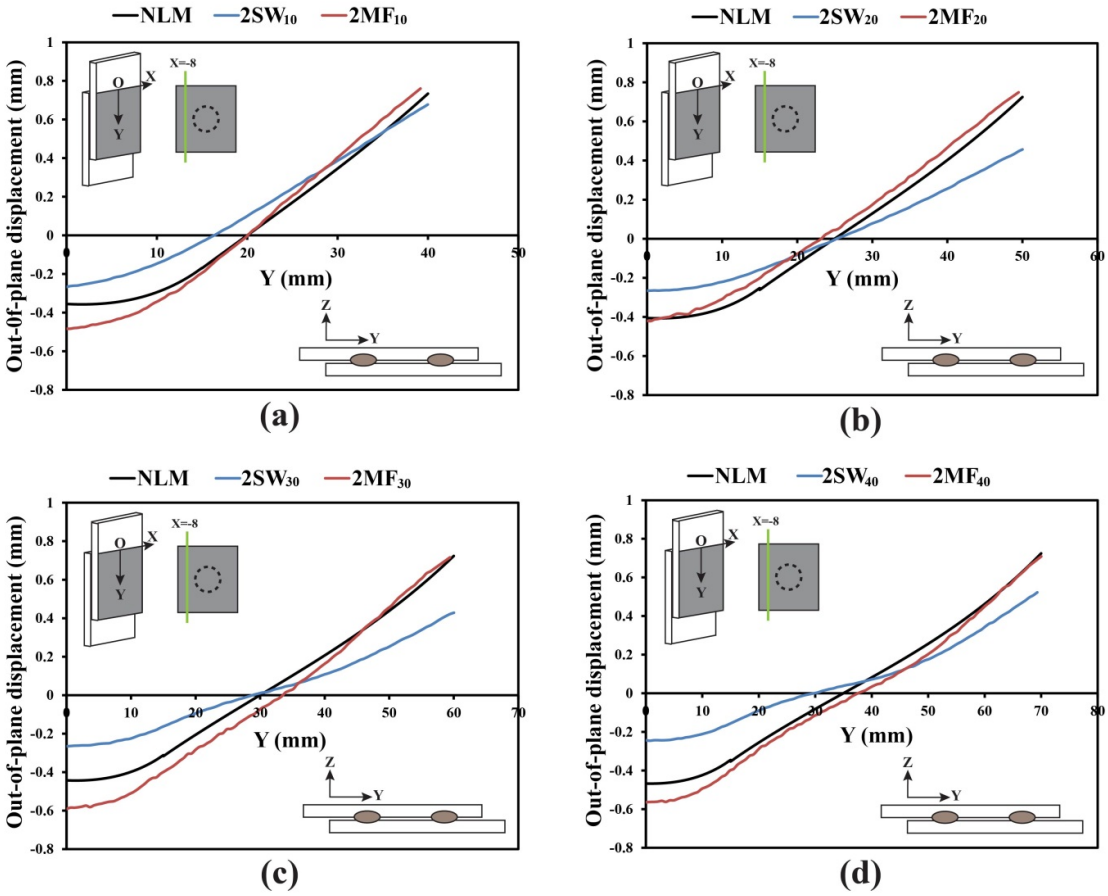

Figure 11. *Out-of-plane displacement as predicted by the neutral line model (NLM), and as calculated from DIC measurements for 2MF and 2SW joints with different inter-row distances: (a) RD=10 mm, (b) IRD=20 mm, (c) IRD=30 mm and (d) IRD=40mm. A maximum load of 5000N was considered / applied in all cases.*

Table 3. *Simplified rotation of the overlap for the 2SW and the 2MF joints as estimated from DIC data plotted in Figure 10 (load 5000 N) for increasing inter-row distance.*

Inter-row distance (mm)	$Tan(\alpha)_{SW}$	$Tan(\alpha)_{MF}$
10	0.024	0.032
20	0.014	0.024
30	0.012	0.022
40	0.011	0.018

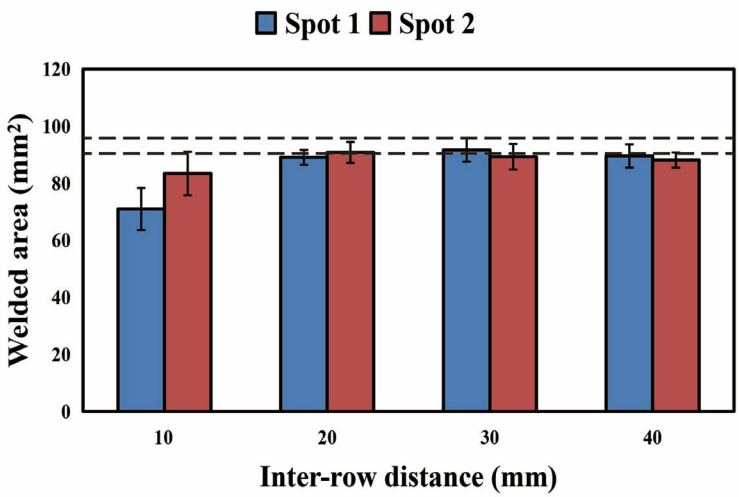

Figure 12. *Average welded areas of each spot in the double-row spot welded joints with increasing inter-row distance. The horizontal dotted lines indicate the average welded area ± standard deviation of the single-row spot welded joints.*

Table 4. *Welded area (WA) for the double-row spot welded joints with increasing inter-row distance.*

Inter-row distance (mm)	WA first spot (mm^2)	WA second spot (mm^2)	Average WA per spot (mm^2)	Average WA per spot/average WA in 1SW joints (%)
10	70.9 ± 7.3	83.4 ± 7.6	77.2	83.3
20	89.0 ± 2.6	90.8 ± 3.6	89.9	97.0
30	91.6 ± 4.1	89.3 ± 4.4	90.5	97.6
40	89.5 ± 4.0	88.1 ± 2.6	88.8	95.8

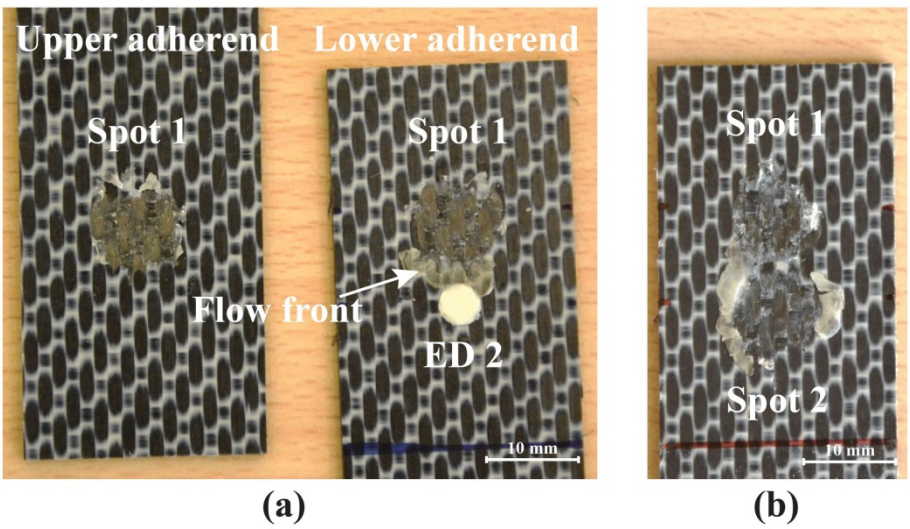

Figure 13. *(a) Mating fracture surfaces obtained after the first step (i.e. welding of the first spot) in creating a double-row spot welded sample (IRD=10 mm). (b) Fracture surface of a double-row spot welded sample (IRD=10 mm) after sequential welding of both spots.*

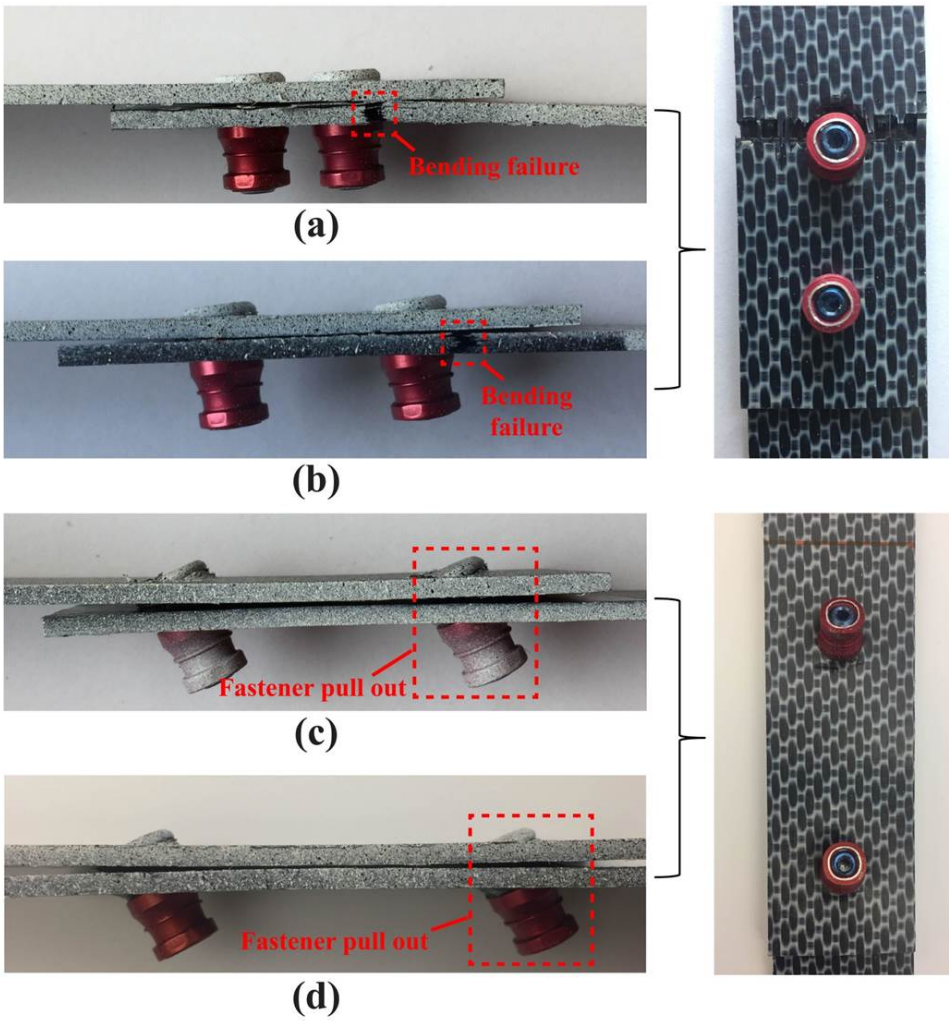

Figure 14. *Different failure types for different IRD values: (a) IRD=10 mm, net section bending failure; (b) IRD=20 mm, net section bending failure; (c) IRD=30 mm, fastener pull out; (d) IRD=40 mm, fastener pull out.*

3.3 Multi-row single lap joints

Increasing the number of rows from one to four in the spot welded and in the mechanically fastened joints gradually increased the load carrying capability of the single lap joints as shown in Figure 15 and in Table 2. The LCC increase was, however, not proportional to the increase in the number of spots or fasteners. The biggest LCC increase was observed when increasing from one to two spots or fasteners and the smallest one when increasing from three to four spots or fasteners. The increase in LCC was in all cases higher for the spot welded joints. Consequently the approximately 10% initial difference in average LCC between single-

row welded joints and mechanically fastened joints (lower LCC for the former) was reduced to virtually zero in the case of four rows of spots/fasteners.

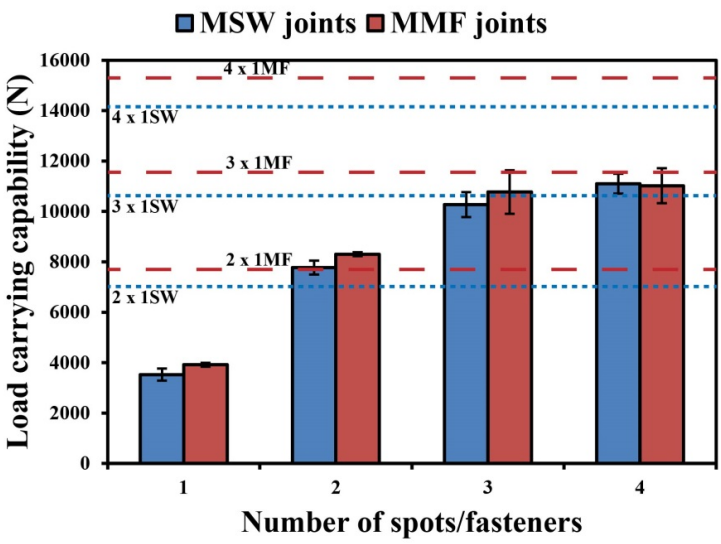

Figure 15. *Load carrying capability of multi-row spot welded and mechanically fastened joints as a function of the number of rows. Note: the samples with 2, 3 and 4 rows have an overlap length of 70 mm. The samples with a single row have an overlap length of 25.4 mm. References corresponding to two, three and four times the LCC of single-row spot welded and mechanically fastened joints are represented as horizontal dotted and dashed lines, respectively.*

The non-linear increase of the LCC for increasing number of rows in the mechanically fastened joints can be explained by the known fact that in joints with more than two rows of fasteners with finite stiffness the load is not evenly distributed among the fasteners. As it is, the outer fasteners carry a higher percentage of the load than the inner fasteners [13, 26-28]. According to the results shown in Figure 15 and Table 2, this, i.e. uneven load distribution, also seemed to be the case in the spot welded joints. The however higher rate at with LCC seem to increase with increasing number of rows for the spot welded joints could probably be explained by differences in secondary bending in both types of joints. The out-of-plane displacement measured for the multi-row spot welded and mechanically fastened joints (see Figure 16) indicated that the overlap rotation (see Table 5) and hence secondary bending decreased with increasing number of welded spots but stayed roughly constant for increasing number of fasteners. Consequently, the loading conditions were more favourable for the spot

welded joints as the number of rows increased. The fact that the same did not happen for the mechanically fastened joints could potentially be explained by the progressive damage in the adherends caused by the increasing number of holes.

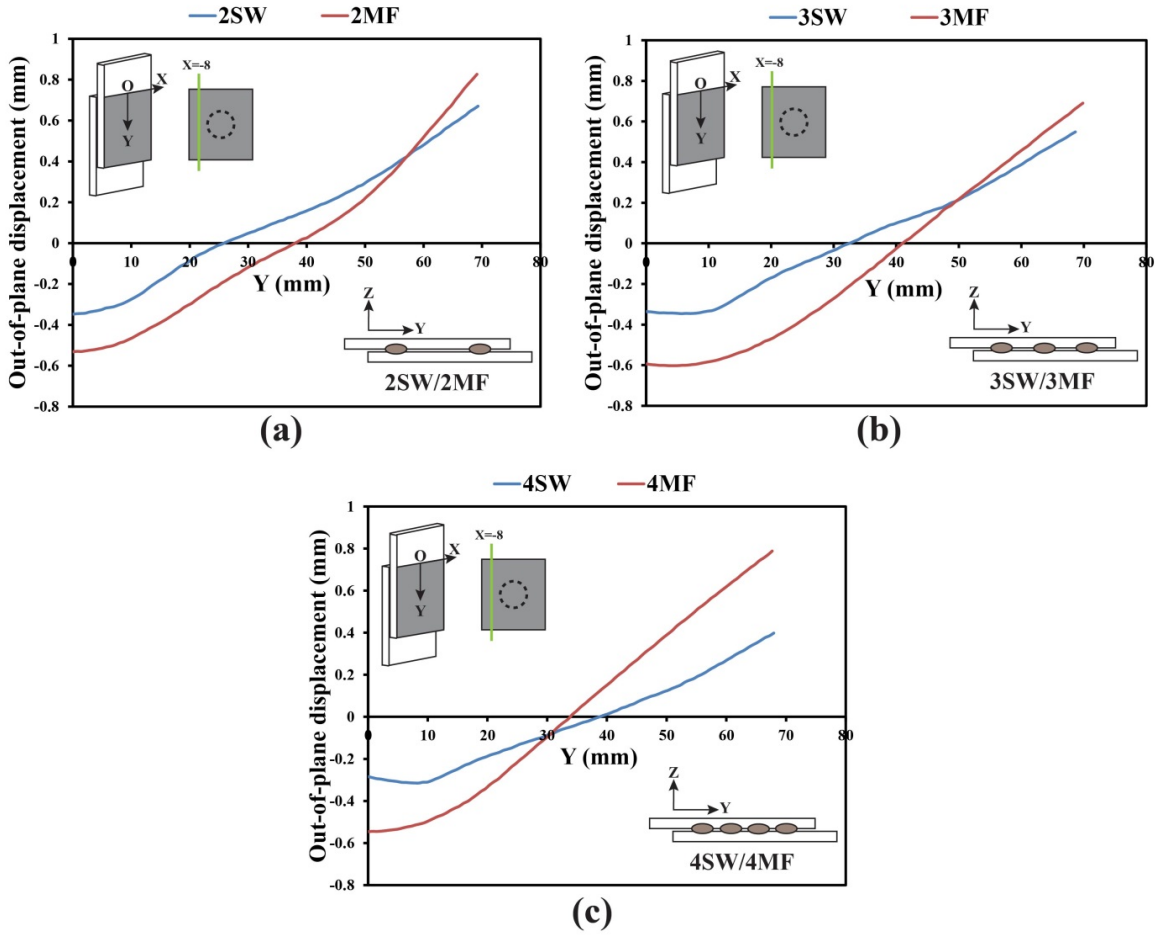

Figure 16. *Out-of-plane displacement in (a) 2SW vs. 2MF,(b) 3SW vs. 3MF and (c) 4SW vs. 4MF joints as calculated from DIC data. A maximum load of 7000N was applied in all cases.*

Table 5. *Simplified rotation of the overlap for the 2SW, 3SW, 4SW, 2MF, 3MF and 4MF joints as estimated from DIC data plotted in Figure 16 (load 7000 N).*

Number of spots/fasteners	$Tan(\alpha)_{SW}$	$Tan(\alpha)_{MF}$
2	0.015	0.020
3	0.013	0.018
4	0.010	0.020

Upon examination of the samples after mechanical testing, first-ply failure was ascertained for all the spot welded joints (see Figure 17). It is interesting to note that owing to

the close distance between the spots in the four-row welded joints the average welded area was lower than in the other cases (see Table 6). This is similar to the case of the double-row welded joints with the shortest inter-row distance and hence attributed to the interaction between molten and unmolten energy directors during the welding process (see discussion in section 3.2). In the case of the mechanically fastened joints, increasing the number of fasteners above two caused a change in the failure type from fastener pull out to net section tension failure (Figure 18).

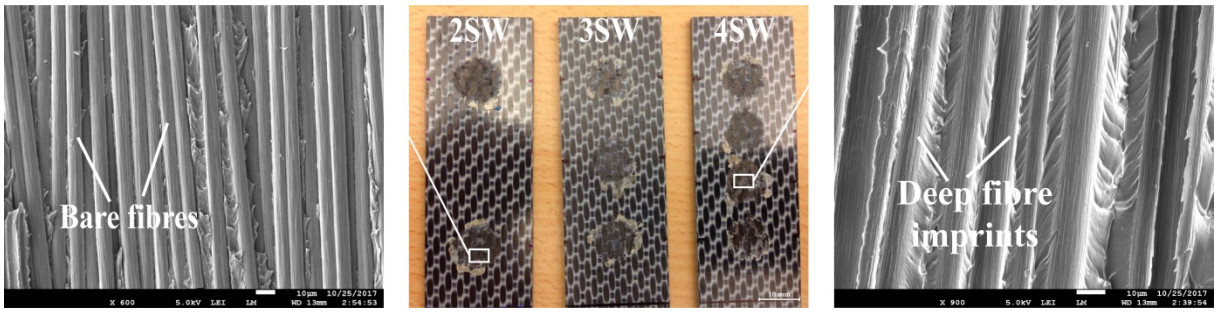

Figure 17. *Representative fracture surfaces for 2SW, 3SW and 4SW joints. SEM details show first-ply failure.*

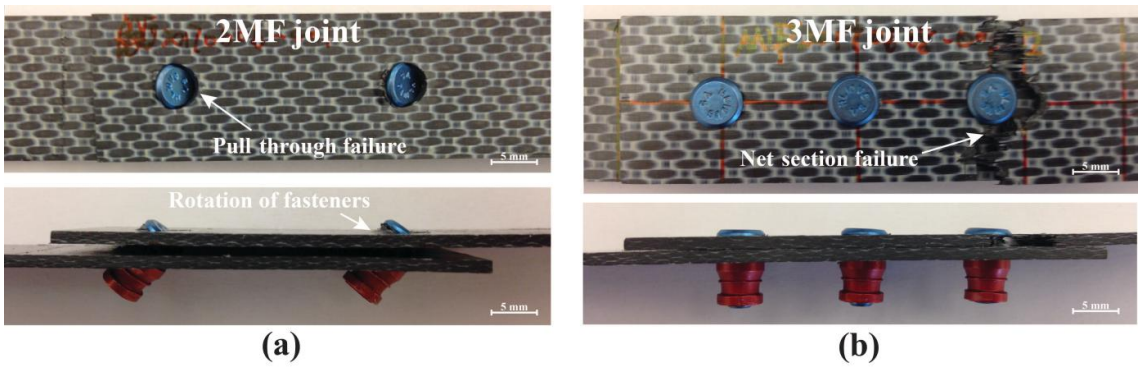

Figure 18. *Change in failure mode with increasing number of fasteners in multi-row mechanically fastened joints: (a) 2MF joints, fastener pull out, (b) 3MF joints, net section tension failure.*

Table 6. *Welded area for the multi-row spot welded joints*

Number of spots	Inter-row distance (mm)	Average WA per spot (mm^2)	Average WA per spot/average WA in 1SW joints (%)
1	-	92.6	100
2	40.0	88.8	95.8
3	20.0	89.8	97.0
4	13.3	81.8	88.3

The above change in failure mode for the mechanically fastened joints brings up a key point of discussion when comparing multi-row spot welded and mechanically fastened joints: the extent of their similarity for design purposes. It is easy to make an analogous comparison between mechanical fastening and spot welding, and it can be tempting to translate numerous design rules-of-thumb, such as constraints on acceptable fastener spacing, row spacing, edge distances, etc. for mechanical fastened joints to spot welded joints, but this will not always be appropriate. Take for example the spacing between fasteners in a typical lap joint. Rules and guidelines for this in mechanically fastened joints are driven by the weakening of the material being joined. The holes remove material, reducing the net section of the material, resulting in an increase in the likelihood of net-section tension failure. This is precisely what occurred in multi-row mechanically fastened tests in this study, where the distribution of load between multiple fasteners shifted the criticality of failure to net-section failure (Figure 18). Here the width of the sample did not change but the load distribution between fasteners increased the criticality of the net-section due to the bypass load in the joint. Many of the design rules-of-thumb in mechanically fastened joints are derived from experience based on the interplay between different failure modes (i.e. net-section tension failure, shear tear-out failure, bearing failure, fastener shear failure, and fastener pull-out failure). It is clear, however, that the criticality or even applicability of each of these failure modes will be different for spot welded joints. In this study, it was observed that eliminating the hole in the joints when welding drastically reduced the criticality of the joints in terms of failure mode. Consequently, it is expected that a greater emphasis on failure of the spot welds themselves rather than on the weakening of the adherends will be crucial to the successful design of multi-spot welded joints.

4 Conclusions

This study aimed at assessing the viability of multi-row spot welding for thermoplastic composite CF/PPS joints in a single-lap configuration. The spot welded joints were created

using sequential ultrasonic welding and their performance under static tensile loading was compared to that of mechanically fastened joints. The main conclusions from the results obtained are the following:

- Despite the significantly lower peel performance of spot welded joints (according to results of our previous study) and the combination of shear and peel loading in single-lap joints, the load carrying capability of multi-row single-lap spot welded joints was not significantly lower than that of the mechanically fastened joints. In particular, the load carrying capability of the spot welded joints was generally 10% lower than that of the mechanically fastened joints for the configurations investigated in this study.
- Considerably higher stiffness of the multi-row spot welded joints, which resulted in lower out-of-plane rotation during mechanical testing of the joints and hence lower secondary bending and peel stresses, was believed to reduce the criticality of peel strength on the overall mechanical performance of the multi-row spot welded joints.
- Similarly to mechanically fastened joints, increasing the distance between rows in double-row spot welded joints was found to increase the load carrying capability of the single-lap joints. Also similarly to mechanically fastened joints, increasing the number of rows above two increased the load carrying capability of the spot welded joints, however the load was not uniformly distributed among the rows which resulted in no significant benefits by increasing the number of welded spots above three.
- Contrarily to mechanically fastened joints, increasing the number of welded spots in a fixed overlap did not weaken the adherends which suggests increased design flexibility in multi-row welded joints. It should be however noted that a too short distance between spots may cause a decrease in the total welded area with a negative impact on the load carrying capability of the welded joint.

- Observations from this study showed that multi-spot welded joints have the potential to compete with mechanically fastened joints. However, design rules and methods commonly used for mechanically fastened joints do not necessarily apply to multi-spot welded joints and hence specific methods should be defined in order to fully exploit their potential.

Acknowledgements

T. Zhao thanks the PhD Scholarship Fund from the China Scholarship Council (CSC) for overseas study and Dr. Wang for his valuable contribution to the discussion. Part of the experimental results presented in this paper were also presented at the 18th European Conference on Composite Materials (ECCM 18), Athens/Greece, 24-28th June 2018.

References

[1] Offringa AR. Thermoplastic composites-rapid process applications.pdf. Composites: Part A: Applied Science and Manufacturing. 1996;27A:329-36.
[2] Ageorges C, Ye L, Hou M. Advances in fusion bonding techniques for joining thermoplastic matrix composites a review. Composites: Part A: Applied Science and Manufacturing. 2001;32:839-57.
[3] Yousefpour A, Hojjati M, Immarigeon JP. Fusion bonding-welding of thermoplastic composites. Journal of Thermoplastic composites Materials. 2004;17:303-41.
[4] Villegas IF. Strength development versus process data in ultrasonic welding of thermoplastic composites with flat energy directors and its application to the definition of optimum processing parameters. Composites Part A: Applied Science and Manufacturing. 2014;65:27-37.
[5] Palardy G, Villegas IF. On the effect of flat energy directors thickness on heat generation during ultrasonic welding of thermoplastic composites. Composite Interfaces. 2016;24(2):203-14.
[6] Senders F., van Beurden M., Palardy G., Villegas I.F. Zero-flow: a novel approach to continuous ultrasonic welding of CF/PPS thermoplastic composite plates. Advanced Manufacturing: Polymer and Composite Science 2016; 2(3-4):83-92.
[7] Zhao T, Palardy G, Villegas IF, Rans C, Martinez M, Benedictus R. Mechanical behaviour of thermoplastic composites spot-welded and mechanically fastened joints: A preliminary comparison. Composites Part B: Engineering. 2017;112:224-34.
[8] Wung P, Walsh T, Ourchane A, Stewart W and Jie M. Failure of Spot Welds under In-plane Static Loading. Experimental Mechanics. 2001;41(1):100-06.
[9] Dieter R, Zheng ZY and Welter M. Local stress parameters at the weld spot of various specimens. Engineering Fracture Mechanics. 1990;37(5):933-51.
[10] Schijve J, Campoli G, Monaco A. Fatigue of structures and secondary bending in structural elements. International Journal of Fatigue. 2009;31(7):1111-23.
[11] Schijve J. Some elementary calculations on secondary bending in simple lap joints. Technical report. National Aerospace Laboratory, Amsterdam; 1972. NLR-TR-72036.

[12] Müller RPG. An experimental and analytical investigation on the fatigue behaviour of fuselage riveted lap joints. The significance of the rivet squeeze force, and a comparison of 2024-T3 and Glare 3. Doctor thesis, Delft University of Technology; 1995.
[13] Ekh J, Schön J, Melin LG. Secondary bending in multi fastener, composite-to-aluminium single shear lap joints. Composites Part B: Engineering. 2005;36(3):195-208.
[14] Ekh J, Schön J. Effect of secondary bending on strength prediction of composite, single shear lap joints. Composites Science and Technology. 2005;65(6):953-65.
[15] Zhao L, Xin A, Liu F, Zhang J, Hu N. Secondary bending effects in progressively damaged single lap, single-bolt composite joints. Results in Physics. 2016;6:704-11.
[16] Fernandez Villegas I, Valle Grande B, Bersee HEN, Benedictus R. A comparative evaluation between flat and traditional energy directors for ultrasonic welding of CF/PPS thermoplastic composites. Composite Interfaces. 2015;22(8):717-29.
[17] Villegas IF, Moser L, Yousefpour A, Mitschang P, Bersee HE. Process and performance evaluation of ultrasonic, induction and resistance welding of advanced thermoplastic composites. Journal of Thermoplastic Composite Materials. 2012;26(8):1007-24.
[18] Dubé M., Chazerain A., Hubert P., Yousefpour A., Bersee H.E.N. Characterization of resistance-welded thermoplastic composite double-lap joints under static and fatigue behaviour. Journal of Thermoplastic Composite Materials 2015; 28(6):762-76.
[19] Zhao T, Broek C, Palardy G, Villegas IF, Benedictus R. Towards robust sequential ultrasonic welding of thermoplastic composites: Welding process control strategy for consistent weld quality. Composites Part A: Applied Science and Manufacturing. 2018; 109: 355-67.
[20] Gamdani F, Boukhili R, Vadean A. Tensile strength of open-hole, pin-loaded and multi-bolted single lap joints in woven composite plates. Materials & Design. 2015;88:702-12.
[21] Hi-Shear. Corporation. Hi-lok®;/hi-Tigue® fastening systems installation instructions. 1991.
[22] Qin T, Zhao L, Zhang J. Fastener effects on mechanical behaviours of double-lap composite joints. Composite Structures. 2013;100:413-23.
[23] de Morais AB, Pereira AB, de Moura MFSF, Silva FGA, Dourado N. Bilinear approximations to the mixed-mode I–II delamination cohesive law using an inverse method. Composite Structures. 2015;122:361-6.
[24] Shi H, Villegas IF and Bersee HEN. An investigation on the strain distribution of resistance welded thermoplastic composite joints. In Proceeding of 53rd AIAA/ASME/ASCE/AHS/ASC Structures, Structural Dynamics and Materials Conference. April 23-26, 2016, Honolulu, Hawaii.
[25] Tencate. Product datasheet: TenCate Cetex® TC1100 PPS resin system. 2016.
[26] Ekh J, Schön J. Finite element modelling and optimization of load transfer in multi-fastener joints using structural elements. Composite Structures. 2008;82:245-56.
[27] Naarayan SS, Kumar DVTGP, Chandra S. Implication of unequal rivet load distribution in the failures and damage tolerant design of metal and composite civil aircraft riveted lap joints. Engineering Failure Analysis. 2009;16: 2255–73.
[28] Taheri-Behrooz F, Shamaei Kashani AR, Hefzabad RN. Effects of material nonlinearity on load distribution in multi-bolt composite joints. Composite Structures. 2015;125: 195–201.